MAUSAM, **77**, 1 (January 2026), 71-82

MAUSAM

DOI: https://doi.org/10.54302/4fm9ar91
Homepage: https://mausamjournal.imd.gov.in/index.php/MAUSAM

UDC No.551.511.33

Spatial variability of sensible and latent heat fluxes with convective thermodynamic indices over East India during pre-monsoon season

ABHEENDRA BANDARY[1, 2], RAJESH KUMAR SAHU[1, 3] and BHISHMA TYAGI [1*]

[1]*Department of Earth and Atmospheric Sciences, National Institute of Technology Rourkela, Rourkela – 769008, India*

[2]*School of Earth, Ocean and Climate Sciences, Indian Institute of Technology Bhubaneswar, Bhubaneswar, Odisha, 752050, India*

[3]*CSIR – Fourth Paradigm Institute, NAL Belur campus, Wind tunnel road, Bengaluru 560037, Karnataka*

(*Received 9 December 2023, Accepted 19 September 2025*)

[*]**Corresponding author's email: tyagib@nitrkl.ac.in**

सार – यह अध्ययन पूर्वी भारत (ओडिशा, पश्चिम बंगाल एवं झारखंड) में पूर्व-मानसून ऋतु के दौरान सर्फ़ेस सेंसिबल हीट फ़्लक्स (SHF), सर्फ़ेस लेटेंट हीट फ़्लक्स (LHF), कन्वेक्टिव अवेलेबल पोटेंशियल एनर्जी (CAPE) तथा कन्वेक्टिव इन्हिबिशन एनर्जी (CIN) की स्थानिक विभिन्नता का 2001-2021 की अवधि के लिए विश्लेषण प्रस्तुत करता है। परिणामों से पता चलता है कि 0900 UTC पर, पूर्वी भारत के आंतरिक भागों में अंतर्देशीय क्षेत्रों में ऊपर की ओर SHF के औसत मान में लगभग 250 से 300 W/m2 तक की वृद्धि हुई| दिन के समय LHF परिवर्तनशीलता उच्च मान दर्शाती है और रात्रि के समय निम्न मान दर्शाती है, तटीय क्षेत्रों में LHF मान -10 से -50 W/m2 तक बढ़ते हुए पाए जाते हैं। मैन-केंडल प्रवृत्ति (MKT) विश्लेषण से पता चलता है कि 0900 यूटीसी पर, पूर्वी भारत के दक्षिण-पश्चिम और उत्तर-पूर्वी भागों में SHF के लिए उच्च सकारात्मक प्रवृत्ति मान लगभग 2-4 W/m2 प्रति मौसम/वर्ष दर्शाते हैं। LHF केवल झारखंड और पश्चिम बंगाल के कुछ भागों में ही इसी सीमा के साथ उच्च सकारात्मक प्रवृत्ति प्रदर्शित करता है। 2100 UTC पर आंतरिक क्षेत्रों में SHF एवं LHF के मान अपेक्षाकृत कम रहे तथा उनकी प्रवृत्तियाँ −0.2 से 0.2 W/m² प्रति ऋतु/वर्ष के मध्य मिश्रित रूप में पाई गईं। SHF-CAPE तटीय क्षेत्रों को छोड़कर अध्ययन क्षेत्र के कई क्षेत्रों में 0900 UTC पर 0.2 और 0.4 के बीच उच्च सकारात्मक सहसंबंध मान दर्शाता है। ओडिशा के अंतर्देशीय क्षेत्रों में 9:00 UTC पर SHF-CIN के लिए 0.1 से 0.2 तक का सकारात्मक सहसंबंध देखा गया, जबकि 21:00 UTC के दौरान उच्च सकारात्मक मान देखे गए। 9:00 और 21:00 UTC पर LHF-CAPE के सहसंबंध मान तटीय क्षेत्रों के लिए सकारात्मक सहसंबंध दर्शाते हैं। लेकिन LHF-CIN के लिए सकारात्मक सहसंबंध 9:00 और 21:00 UTC के दौरान तटीय क्षेत्रों में और 21:00 UTC के मामले में अंतर्देशीय क्षेत्रों में देखा गया।

ABSTRACT. This study investigates the spatial variation of surface sensible heat flux (SHF) and surface latent heat flux (LHF), along with the Convective Available Potential Energy (CAPE) and Convective Inhibition Energy (CIN), during the pre-monsoon season over East India (states of Odisha, West Bengal, and Jharkhand) from 2001-2021. The results reveal that at 0900 UTC, the mean values of upward SHF increased over the inland regions in the interior parts of East India, ranging from approximately 250 to 300 W/m^2. At 2100 UTC Inland regions of Odisha and Jharkhand experiences downward SHF with values ranging between 15-20 W/m^2. The LHF variability shows high values during the daytime and low values during the nighttime, with coastal regions exhibiting upward LHF values ranging from -10 to -50 W/m^2. The Mann-Kendall trend (MKT) analysis indicates that at 0900 UTC, southwest and northeast parts of East India show high positive trend values for SHF, approximately 2-4 W/m^2 per season/year. LHF exhibits a high positive trend in only a few parts of Jharkhand and West Bengal, with a similar range. At 2100 UTC, lower SHF and LHF values are present over the interior regions, displaying mixed trend patterns ranging between -0.2 and 0.2 W/m^2 per season/year. SHF–CAPE demonstrates higher positive correlation values, ranging between 0.2 and 0.4 at 0900 UTC in many regions

of the study area except coastal regions. At 2100 UTC majority of the regions exhibit negative correlation values. Inland regions of Odisha exhibit positive correlation for SHF–CIN at 0900 UTC, ranging from 0.1 to 0.2, while higher positive values were observed during 2100 UTC. The correlation values of LHF-CAPE at 0900 and 2100 UTC show positive values for coastal regions. But for LHF-CIN positive correlations are seen for coastal regions during 0900 and 2100 UTC and for inland regions in case of 2100 UTC.

Key words – Heat flux, Mann-Kendall test, East India, CAPE, CIN.

1. Introduction

Temperature and humidity are the primary drivers of any convective event (Braham, 1952; Samanta *et al.*, 2020). Surface energy fluxes directly impact surface temperature, humidity, and the thermodynamic behaviour of the atmosphere (Tyagi *et al.,* 2012). Sensible heat flux (SHF) and latent heat flux (LHF) characterize the turbulent exchange of heat between the land surface and the atmosphere (Laird & Kristovich, 2002; Tyagi *et al.*, 2014). Latent heat in the atmosphere primarily arises from two main contributors: evaporation and evapotranspiration, driven by vapour pressure gradients (Nordbo *et al.,* 2011; Martínez-Alvarez *et al.,* 2011). The distribution of sensible and latent heat at the ground surface offers insights into the strength of the interaction between the atmosphere and the land (Martens *et al.,* 2020). Approximately half of the energy in the atmosphere is derived from water vapour, provided through latent heat, thus, connecting the energy budget to the water cycle (Garstang, 1967). Surface SHF plays a pivotal role in heat generation and has garnered significant attention recently (Yang *et al.,* 2011). Sensible heating contributes to the initiation of convection, making it essential to investigate surface fluxes to comprehensively understand convective activity (Keenan *et al.,* 1994; Satyanarayana *et al.,* 2014).

Surface heat fluxes have been studied over various regions, *e.g*., Duan and Wu (2009) and Chen *et al.* (2014) found a decrease in SHF and an increase in LHF over the Tibetan Plateau over the years. (Benítez-Valenzuela and Sanchez-Mejia 2020) highlighted the sensitivity of SHF during the pre-monsoon and monsoon seasons, as well as LHF during the pre-monsoon season near the coastal lagoon of the Gulf of California. Over the Indian region, Tyagi and Satyanarayana (2015) examined fluxes over Ranchi, revealing that SHF dominates from sunrise to sunset on days without convective activity, whereas both fluxes have similar magnitudes on days with thunderstorms. Gogoi *et al.* (2019) observed notable changes in LHF and SHF when plant levels increased in the Odisha region, reducing land surface temperature. A study conducted at an Indian Council of Agricultural Research (ICAR) farm in Delhi, India, found that during the pre-monsoon season, SHF exceeds LHF, while during the monsoon season, the opposite pattern is observed (Danodia *et al.,* 2018).

The occurrence of thunderstorms not only changes the surface fluxes but also marks significant variations in the vertical atmosphere (Tyagi *et al.,* 2011). The most common thermodynamic indices used to comprehend the progression of convection in any region are Convective Available Potential Energy (CAPE) and Convective Inhibition (CIN) (Murugavel *et al.,* 2014; Westermayer *et al.,* 2017). Riemann-Campe *et al.,* (2009) presented global climatology of CAPE and CIN, highlighting that significant mean climatological CAPE values are found over the ITCZ, while large CIN values are observed in the subtropics. DeMott & Randall, (2004) mentioned that multi decadal trends of CAPE where positive trend is shown in Caribbean Sea and western Pacific Ocean. Meanwhile (Zhang, 2002) mentioned that CAPE changes are mainly driven by boundary layer processes rather than free tropospheric using modified quasi-equilibrium assumption for midlatitude continental convection. (Murugavel *et al.,* 2012) showed that during the pre-monsoon season and monsoon season over India there exists a belt of high CAPE along east coast and southeast coast over India. Previous studies like (Murthy & Sivaramakrishnan, 2006), (Bhat, 2001) studied CAPE trends across various regions of India but only for short durations, such as two months or one year (Roy Bhowmik *et al.,* 2008) but not for longer period. Sahu *et al.* (2022a) provided insights into convective indices, seasonal variations, and trend analysis over the East India region during the pre-monsoon season for 20 years period. Despite East India's susceptibility to various convective-related natural disasters, there is a lack of studies regarding fluxes in this region. Therefore, the primary objective of this study is to comprehend the spatial variations in surface energy fluxes and their correlation with convective indices in East India. This study aims to analyze both the mean and trend variations using the Mann-Kendall Test for flux and thermodynamic variables during the pre-monsoon season. Additionally, it seeks to emphasize the spatial correlations between fluxes and thermodynamic variables.

2. Data and methodology

2.1. *Study area*

The study area for the present work comprises of three states Odisha, Jharkhand, West Bengal, as portrayed

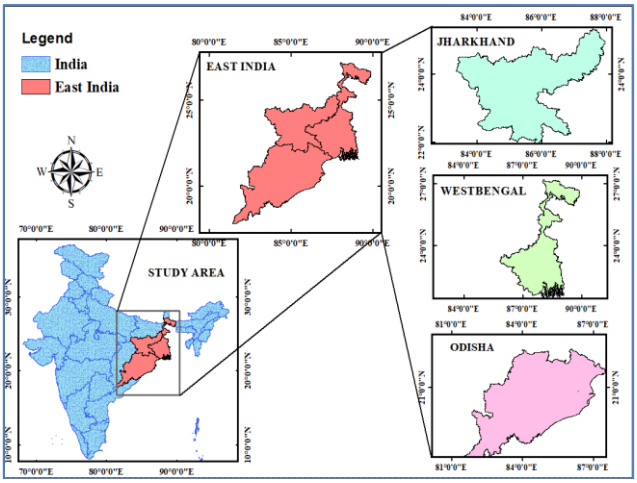

Fig. 1. Study region, East India with states Odisha, West Bengal, and Jharkhand with their respective locations in India

in Fig. 1, termed as East India. In the pre-monsoon season (March - May), the region encounters frequent thunderstorms called as 'Kal Baisakhi' or Nor'westers (Sahu *et al.*, 2020a; Sahu *et al.*, 2020b; Tyagi *et al.*, 2022). The state of Odisha is on the shoreline which is nearly 480 km at the head of the Bay of Bengal (Patnaik *et al.*, 2013). In accordance with the Koppen's Climate Classification, it falls under '*Aw*' which implies both tropical dry and wet and is sometimes called tropical savanna climate (Peel *et al.*, 2007). West Bengal is situated alongside Odisha, with some districts directly encountering the Bay of Bengal. The state is bordered by Assam, Jharkhand, Odisha, *etc*. among other different states. The Koppen's climate classification 'Aw' and 'As' describes the state's climate as humid subtropical in the north and in case of the south, it is tropical savanna. Adjoining Odisha and West Bengal, Jharkhand state, also known as "The land of forest", is also part of our study area. According to Koppen's classification of climate, Jharkhand has a tropical dry and wet climate (Aw and As) in the south-east and a humid subtropical climate in the North.

2.2. *Methodology*

The present study utilizes European Centre for Medium-Range Weather Forecast (ECMWF) reanalysis data, ERA5, at two different times: 0900 UTC (2:30 PM local time) and 2100 UTC (2:30 AM local time), from 2001-2021 pre-monsoon months (March-May). ERA5, the fifth generation ECMWF reanalysis, incorporates data from the last four to seven decades of global climate and weather information (Hersbach *et al.*, 2020). It is distinguished by its use of 137 vertical levels, a feature that sets it apart from other available reanalysis products (Gensini *et al.*, 2021). When compared to previous reanalysis products, ERA-5 data excels in its ability to accurately determine various meteorological parameters such as maximum and minimum temperature, dewpoint temperature, and others across different regions of the world (Mahto and Mishra, 2019). ERA5, like other reanalysis products, has certain limitations when it comes to the Indian region. However, its precise estimation of a wide range of meteorological parameters within the gridded region provides strong motivation for its use in the current research (Sahu *et al.*, 2022b).

2.3. *Spatial correlation*

A measure of a monotonic connection between two variables is defined as correlation, and if done spatially between the two variables it is called spatial correlation. A monotonic connection between two variables is one in which either (*a*) the other variable's value increases as the first variable's value increases, or (*b*) the other variable's value decreases as the first variable's value increases (Schober & Schwarte, 2018). The intensity and direction of the relationship between two variables are indicated by correlation coefficients. The stronger the relation is, the higher the Pearson correlation coefficient's (*r*) absolute value. In the present scenario we have considered a minimum of 30 samples as a must for the correlation to occur. The correlation coefficient is calculated using

$$r = \frac{\frac{1}{n-1}\sum_{j=1}^{n}[(x_j-\bar{x})(y_j-\bar{y})]}{\sqrt{\frac{1}{n-1}\sum_{j=1}^{n}(x_j-\bar{x})^2}\sqrt{\frac{1}{n-1}\sum_{j=1}^{n}(y_j-\bar{y})^2}} \quad (1)$$

Here x_j and y_j represent the timeseries values from different variables at i^{th} and j^{th} grid point respectively and the $\bar{x}$ and $\bar{y}$ represets the averages of the variables timeseries. Stippling is done at 95% significance level using t-test (Fisher, 1992) where the test statistic differs which is given by

$$t = \frac{r\sqrt{n-2}}{\sqrt{1-r^2}} \quad (2)$$

where r is correlation coefficient and n is the number of samples.

2.4. *Mann-Kendall test*

In the present analysis the Mann-Kendall trend (MKT) test is used, which is one of the most popular distribution-free tests for trend analysis (Mann, 1945). The benefit of distribution-free tests is that the actual data distribution has no bearing on their power or significance (Hamed, 2009). This contrasts with parametric trend tests that make the assumption that the data follows the Normal distribution, such as the regression coefficient test (Matalas & Sankarasubramanian, 2003). The traditional MKT makes the fundamental assumption that the data is uniformly

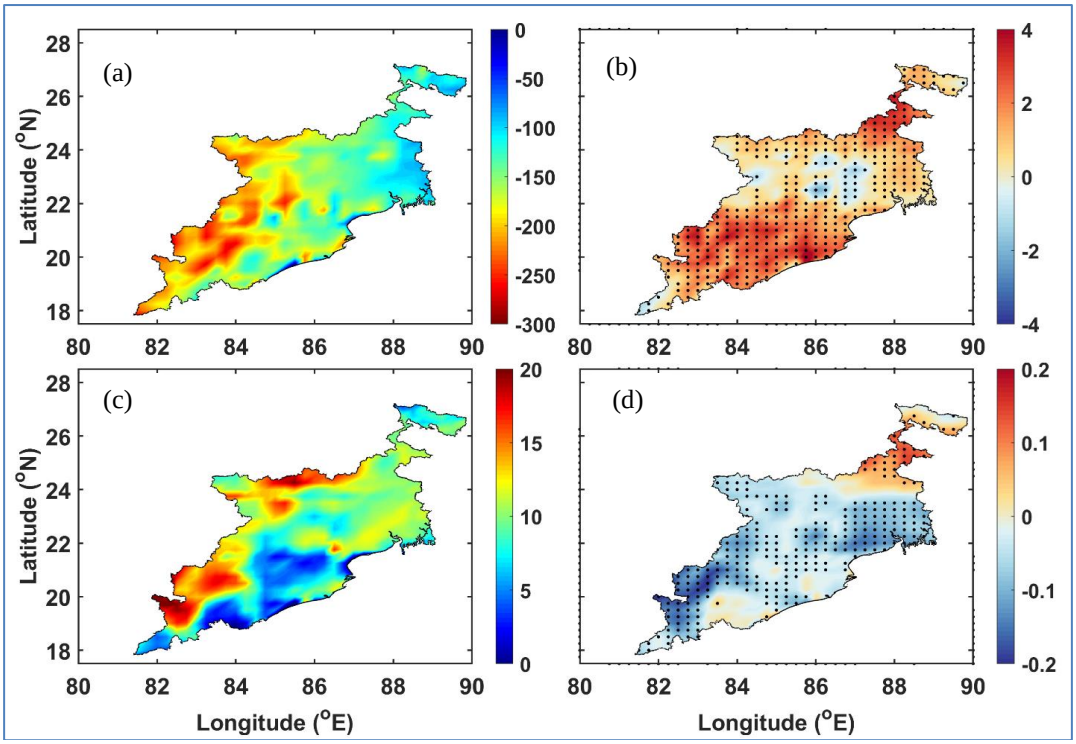

Figs. 2(a-d). SHF mean spatial variation for (a) 0900 UTC, (c) 2100 UTC and MKT analysis for (b) 0900 UTC, (d) 2100 UTC

distributed and arbitrary, which is rarely the case in real-world time series (Hamed, 2009). When several stations are examined in a single study, the MKT is preferred (Hirsch *et al.*, 1991). MKT, non-parametric statistical test, applied in the present work at 95% significance level ($p<0.05$). It acknowledges the absence of any monotonic patterns in a time series as the null hypothesis, and pattern values can be either positive or negative (Vissa and Tyagi, 2021). Sen slope is used to obtain the trend values (Sen, 1968). When a set of observation are present for X where X = x_1, x_2, x_3…, x_n then the statistic is formulated as

$$S = \sum_{i<j} a_{ij} b_{ij} \tag{3}$$

where,

$$a_{ij} = \operatorname{sgn}(x_j - x_i) = \begin{cases} 1 & x_j < x_j \\ 0 & x_j = x_i \\ -1 & x_j > x_j \end{cases} \tag{4}$$

If Y values are the time series for the associated X values then we can consider then it would be a trend test (Mann, 1945). Now the statistic in this case is given as

$$S = \sum_{i<j} a_{ij} = \sum_{i<j} \operatorname{sgn}(x_j - x_i) \tag{5}$$

In order to identify the significance of the trends the standardized test statistic which is Z is compared with the standard normal variate of the required or given significance level (Hamed & Ramachandra Rao, 1998), Where the Z test statistic is given by

$$Z = \frac{S}{\sqrt{Var(S)}} \tag{6}$$

$$\text{Var(S)} = \frac{n(n-1)(2n+5)}{18} \tag{7}$$

The Sen slope is calculated using Sen's non-parametric trend estimator as given by

$$median\ (\frac{x_j - x_i}{j-i})\ \forall\ i<j \tag{8}$$

3. Results and discussion

3.1. *Spatial variability and trend analysis of SHF, LHF, CAPE and CIN*

The provision of energy fluxes from the surface is linked to the commencement of the thunderstorms (Tyagi & Satyanarayana, 2015). We started looking into the variable's thermodynamic indices (CAPE and CIN) and flux variables (SHF and LHF). Fig. 2 shows the mean and trend values for SHF at 0900 and 2100 UTC, representing the daytime upwards (negative values) and nighttime downward motions (positive values) over the study region. SHF values in Fig. 2 exhibit lower values at 0900

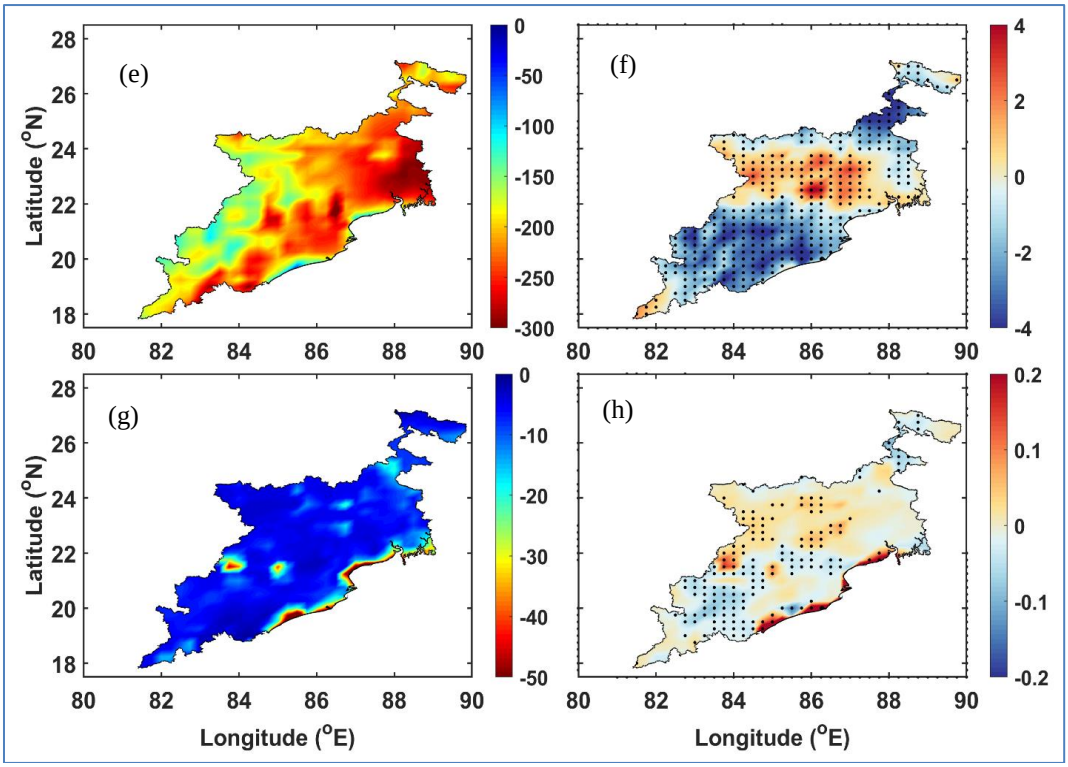

Figs. 3(e-h). LHF mean spatial variation for (e) 0900 UTC, (g) 2100 UTC and MKT analysis for (f) 0900 UTC, (h) 2100 UTC

UTC (The 0900 UTC is the time associated with more convection is expected) (Panel A) over coasts and regions adjacent to the coasts (-50 – -120 W/m^2) and high values (-230 – -320 W/m^2) at further inland. Gogoi *et al.* (2019) suggested that an increase in the SHF is observed favoring the warming of regions of Eastern Odisha, along with that the trend values of NDVI are also very low during pre-monsoon season. Meanwhile (Chakraborty *et al.,* 2021) mentioned that a strong temperature gradient present between the interior and coastal regions especially in the Odisha from west to east (which is again consistent with the strong specific humidity) where western portion is much warmer that eastern portion of Odisha in pre-monsoon season. This could be the reason for the observed increase in the SHF in the present case. Whereas in the case of coasts and adjacent coastal regions the values are lower than mentioned previously. MKT analysis (Panel B) displays the sections of Odisha and parts of West Bengal with higher positive trend values (~ 4 W/m^2 per season/year) for SHF at 0900 UTC. An increase in the trend of surface temperature from 1991 – 2010 was observed by (Gogoi *et al.,* 2019). Whereas parts of Jharkhand and West Bengal demonstrate low trend values (~ -2 W/m^2 per season/year). Tirkey *et al.* (2018) mentioned that a positive trend is observed for maximum temperature in the northwestern parts of Jharkhand with a moderate positive trend values in the northern and southwestern parts. However, at 2100 UTC (Panel C), inland regions show (10–18 W/m^2), but coastal areas exhibit values between (-5–5 W/m^2). SHF shows negative trend patterns (as shown in Panel D) for many regions of Odisha, Jharkhand and mixed trend pattern are observed in different parts of West Bengal at 2100 UTC (~ -0.2–0.2 W/m^2 per season/year). This is to be expected as the SHF is very less due to very little Short-Wave Radiation (SWR) at 2100 UTC. But interestingly, SHF, for NE parts of West Bengal are showing lower positive trend values ranging between (~ 0.05–0.2 W/m^2 per season/year) which still needs to be explored. Land Use Land Cover (LULC) also plays a major role as the increase (decrease) in the built-up areas leads to more SHF (LHF). LHF variability has been shown in Fig. 3, with mean and trend values at 0900 and 2100 UTC, representing the daytime upwards motions (negative values) and nighttime downward motions (positive values) over the study region. The LHF values in (Panel E) exhibit higher values in regions vicinity to the coasts (-250 – -350 W/m^2) at the coastal (West Bengal, Odisha and parts of Jharkhand) and further inland regions (Odisha and Jharkhand interiors) and very near coastal regions show lower values (-90 – -150 W/m^2) at 0900 UTC. This increase in the LHF could be because of the land-sea contrast where moisture is brought from sea to land and gets evaporated which could lead to release in the latent heat. Interestingly the pattern

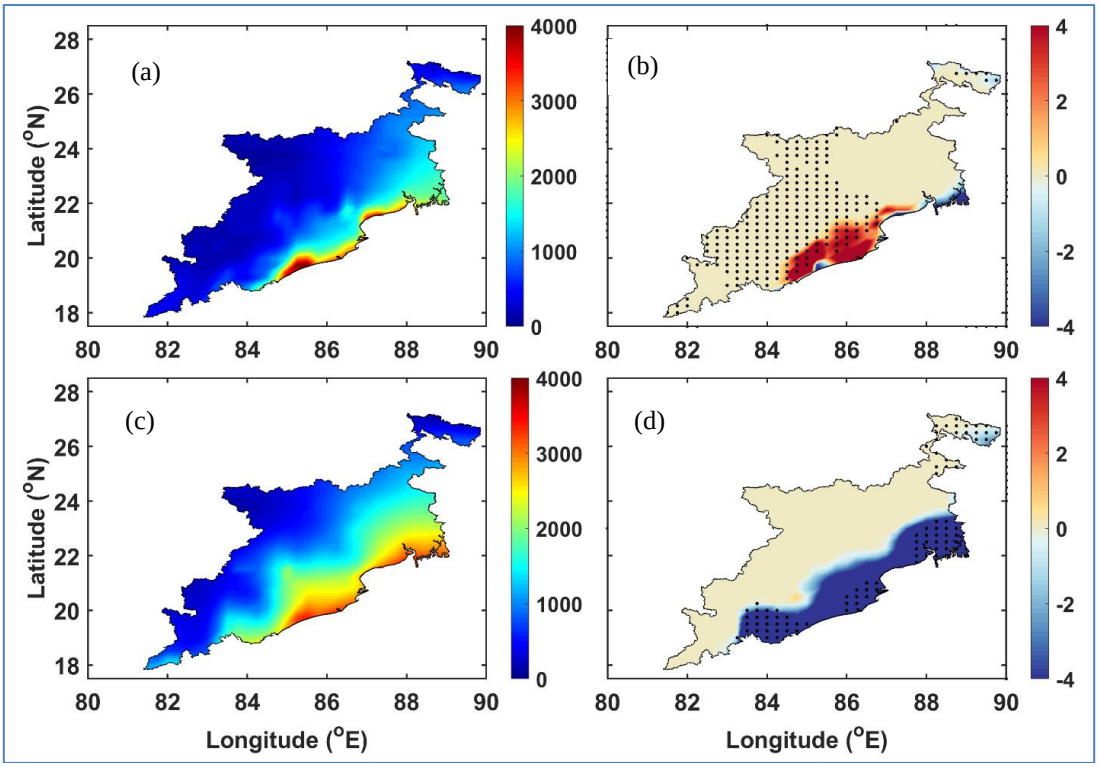

Figs. 4(a-d). CAPE mean spatial variation for (a) 0900 UTC, (c) 2100 UTC and MKT analysis for (b) 0900 UTC, (d) 2100 UTC

here is nearly opposite to the SHF pattern at same UTC. Higher LHF regions in the Odisha are associated in the swamp regions as mentioned by Gogoi *et al.* (2019), which could also lead to an increase in the LHF. LHF trend (Panel F) exhibits higher trend values for parts of Jharkhand and West Bengal (~ 4 W/m^2 per season/year), but negative trend values are shown in other regions (~ -4 W/m^2 per season/year) and is almost opposite the SHF trend pattern as observed over most regions of Odisha and some regions of West Bengal. At 2100 UTC (Panel G), the regions near the coasts exhibit high values of flux (-30 – -50 W/m^2), but as moved further inland, the values start to descend with values between (-10 – 2 W/m^2). Here even at 2100 UTC the SWR is absent, yet LHF is seen upwards (negative values) especially the regions very adjacent to coasts. For LHF at 2100 UTC, the trend pattern (Panel H) is near zero for many regions with lower significance levels (~ -0.2 – 0.2 W/m^2 per season/year). While the trend values are positive and high at coastal regions but as moved to inland regions the magnitude decreases.

Ghosh *et al.* (2004) suggested that strong convective instability along with high moisture availability at lower leels with triggering mechanisms are responsible for thunderstorm development. Instability indices like CAPE and CIN are helpful while accessing the behaviour of convective systems. As mentioned by Arora *et al.* (2023), CAPE is an index that signifies atmospheric instability throughout its depth. which helps in quantifying the intensity of updrafts in the event of a developing convective system. Fig. 4 portrays the CAPE at 0900 (Panel A), which reveals a decreasing pattern while moving from coastal regions exhibiting higher values (2500–3800 J/kg) to further Inlands showing lower values (100–900 J/kg). Inland regions display a trend close to zero for trend values of CAPE at 0900 UTC (Panel B). Sahu *et al.* (2022a) mentioned that CAPE values are positive over the coastal regions and the magnitude decreased as moved to inland regions at 0000 and 1200 UTC. The coastal regions show a mixed pattern involving both positively high (~ 4 J/kg per season/year) and negative low trends (~ -2 J/kg per season/year) with significance in coastal parts of Odisha and West Bengal. For 2100 UTC (Panel C), a similar pattern is observed where coastal and adjacent coastal regions vary in values (2000–3500 J/kg), with the only difference being the area covered. In the case of 2100 UTC trends (Panel D), most inland regions oscillate at zero vicinity, but the coastal and adjacent areas exhibit a considerable negative trend (~ -13 J/kg per season/year). CAPE is modulated by moisture and surface temperature (Gutzler, 1992). Hughes & Veron (2018) suggested that the primary driving mechanism for sea breeze is the temperature gradient between land and ocean, resulting in alterations in atmospheric pressure and humidity of air parcels, thereby creating a circulation cell perpendicular to the coast with

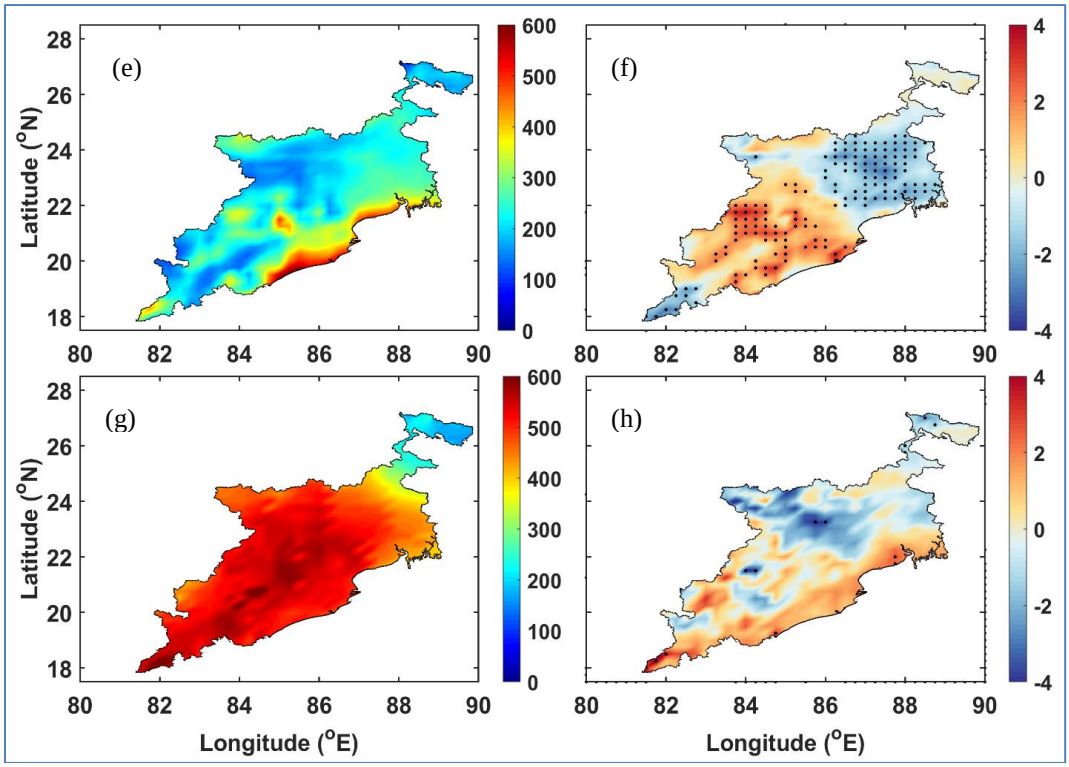

Figs. 5(e-h). CIN mean spatial variation for (e) 0900 UTC, (g) 2100 UTC and MKT analysis for (f) 0900 UTC, (h) 2100 UTC

diurnal variation. This leads to the influx of water vapor from sea onto land. This would lead to an increase in the Relative Humidity over the coastal regions. Which in turn increases the CAPE values, especially regions adjacent to coasts and this decreases as we further move into inland.

CIN shows a similar variability (Fig. 5) as CAPE at 0900 UTC (Panel E) with high values at coastal and adjacent to coastal regions (400-600 J/kg) and experiences a descent as one move further inland. In general, higher CAPE values represent lower CIN values but here besides CAPE, CIN values are also increasing. At 2100 UTC (Panel F) the values exhibit higher CIN values at west and southwest (400–650 J/kg) and descend towards the northwest which is an interesting result. The CIN values trends at 0900 UTC (Panel G), shows a mixed trend pattern where most of the regions of Odisha show a high positive trend (~ 2–4 J/kg per season/year). Still, parts of Jharkhand and West Bengal are more closely associated with trend zero or negative with lower significance (Jharkhand). However, at 2100 UTC CIN trends (Panel H), the coastal regions and parts of Odisha show a positive trend (1–3 J/kg per season/year), while most areas in East India show a low trend or less significance overall. Similar kind of results were observed for CAPE and CIN values by Sahu *et al.* (2022b) at 0000 and 1200 UTC especially for CAPE, while CIN values are showing as decreasing trend from coastal regions to inland regions only at 0900 UTC.

3.2. *Spatial correlation between fluxes and thermodynamics variables*

Fig. 6 shows the spatial correlations between SHF–CAPE and LHF–CAPE for the study period. At 0900 UTC (Panel A), most regions exhibit higher positive correlation values ranging between 0.2–0.4 for SHF–CAPE, although coastalregions exhibit negative values between -0.1– -0.3. This might be because even though there are higher CAPE values, the SHF values displayed are lower (dominant). Nearly all regions exhibit negative correlation for SHF–CAPE at 2100 UTC (Panel B), with values ranging from (-0.1 – -0.4), while only a few locations exhibit slightly positive correlation leveling between (0.1-0.2). This could be because at the places where SHF is increasing CAPE is decreasing and is vice-versa in the other places (most). When it comes to LHF–CAPE at 0900 UTC (Panel C), inland regions show a negative correlation with values ranging from -0.4 – -0.1. Nonetheless, coastal areas exhibit a minimal positive correlation with a maximum value of 0.2. The increase could be attributed to the increase observed for respective variables LHF and CAPE. A similar pattern is observed in the case of the SHF at 0900 UTC. However, the correlation response of

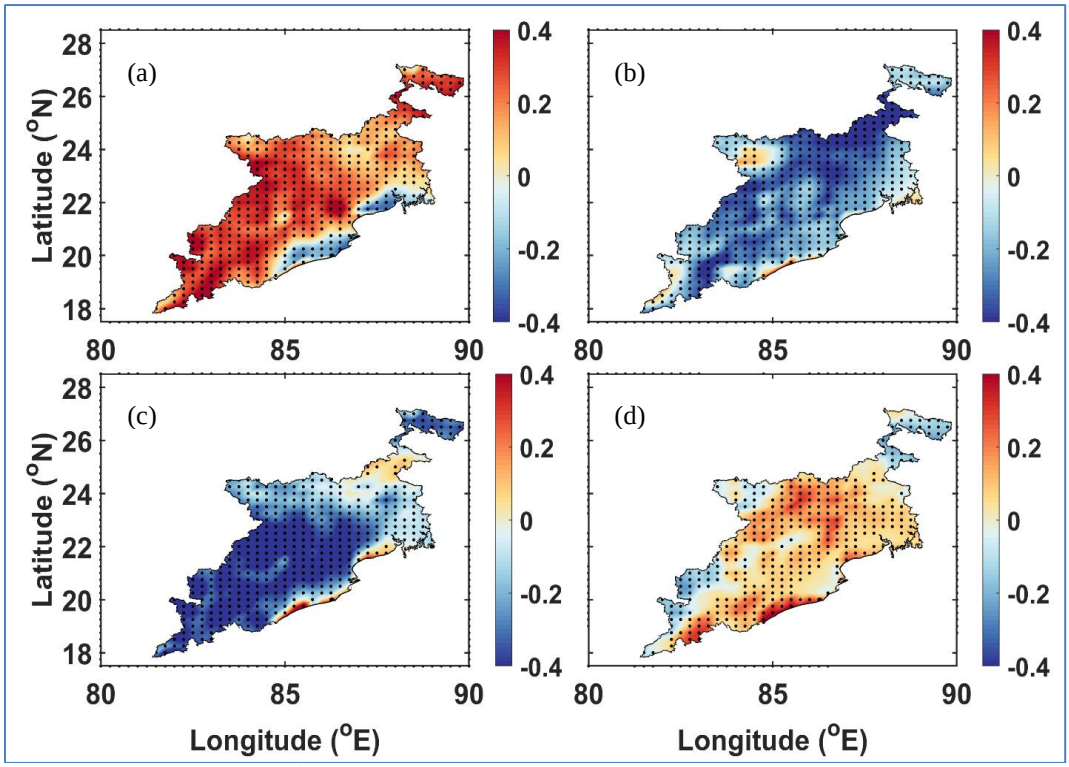

Figs. 6(a-d). Spatial Correlation of SHF–CAPE at (a) 0900 UTC, (b) 2100 UTC, and LHF–CAPE at (c) 0900 UTC, and (d) 2100 UTC

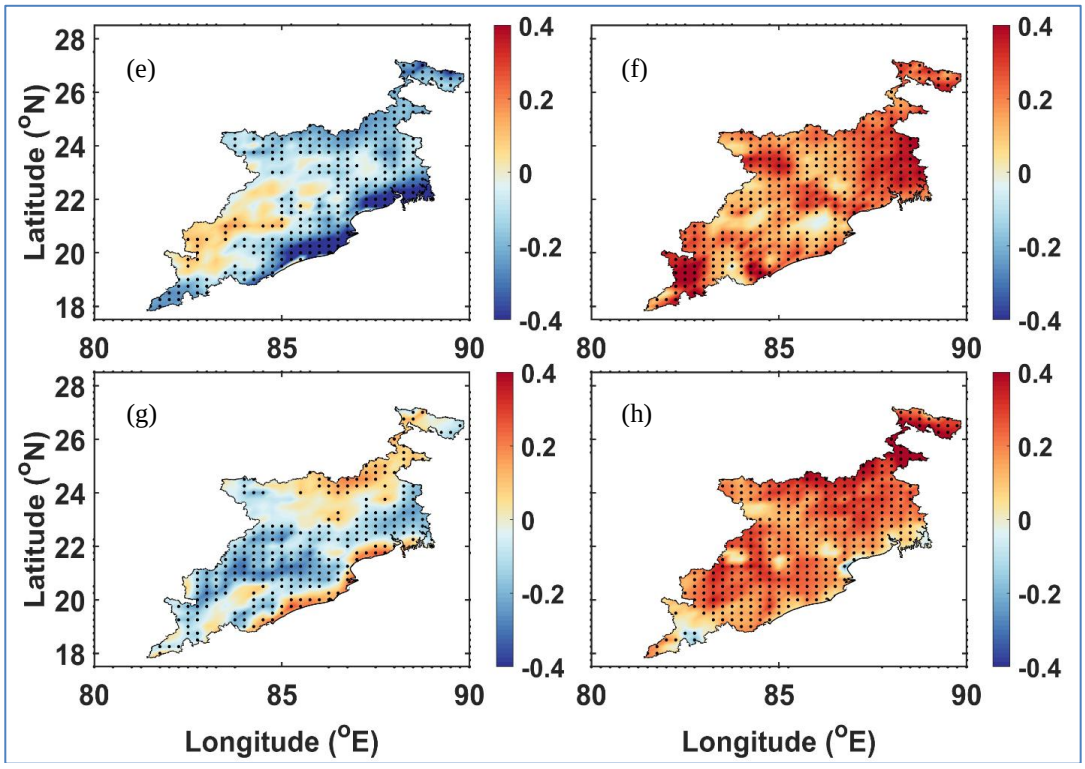

Figs. 7(e-h). Spatial Correlation of SHF–CIN at (e) 0900 UTC, (f) 2100 UTC, and LHF–CIN at (g) 0900 UTC, and (h) 2100 UTC

LHF–CAPE is insignificant at 2100 UTC (Panel D), with values ranging between -0.2 – 0.3, most inner most regions showing a negative correlation. The lower positive correlation can be seen mostly in the parts of West Bengal and Jharkhand and also in Odisha. Higher positive correlation values (0.2 – 0.4) are observed over coastal regions. And vice versa is observed over inland regions in the similar fashion as climatologies of CAPE and LFH are gradually decreasing.

With values ranging from 0.2 to 0.4, inland regions (Odisha) show a positive correlation for SHF–CIN (Panel E) at 0900 UTC. This might be because of the higher values of the SHF (could also be because the CIN values are low). Meanwhile coastal and several other regions show a negative correlation value ranging from -0.4 – -0.1, as the CIN values are higher at coastal regions, but the SHF values are decreasing. Some parts of West Bengal and Odisha are experiencing zero correlation values as well, which shows that the SHF might not be particularly related to CIN variability. SHF–CIN at 2100 UTC (Panel F) overall positive correlation values ranging between 0.2 – 0.4, in most of the regions. For the case of LHF–CIN at 0900 UTC (Panel G) lower correlation values are observed for the inland regions with values ranging between -0.1 – -0.3. Parts of Odisha along with coastal regions, Jharkhand and West Bengal are experiencing positive correlation with values ranging between 0.1-0.3. The results suggest that the LHF does not show an impact on CAPE and CIN at 0900 UTC over the region except some parts and for the coastal regions. For the LHF–CIN at 2100 UTC (Panel H), spatial correlations show an improvement in the correlation values in most of the regions with values ranging between 0.1–0.4. The south most Odisha regions along with some interior regions of West Bengal and Jharkhand shows either zero or negative correlation values ~ 0.1. This is again an interesting result because the CIN values are increasing most of the Eastern India, but SHF values are decreasing as moved from coastal to inland regions.

4. Conclusions

The primary objective of this study is to analyze the variability of SHF and LHF over East India. As the study experiences frequent thunderstorm occurrences during the pre-monsoon season, correlations of SHF and LHF with CAPE and CIN may be insightful for understanding the flux relations with thermodynamics. The findings can be summarized as follows:

(*i*) The spatial variations of SHF show that values at 0900 UTC are low over coasts and regions adjacent to the coasts (50–120 W/m^2) and higher (230–320 W/m^2) for inland regions. For 2100 UTC, the values are reduced to 10–18 W/m^2 (inland regions), and 0–5 W/m^2 (coastal areas). The LHF exhibits higher values at 0900 UTC of -250 – -350 W/m^2 (near coasts) and lower values (-90 – -150 W/m^2) for inland regions. The values reduced during 2100 UTC, with higher near coastal flux (-30 – -50 W/m^2), and values between -10 – 2 W/m^2 over inland regions.

(*ii*) Trend analysis for SHF shows that certain regions of Odisha and West Bengal have significantly positive trend values (~ 4 W/m^2 per season/year) at 0900 UTC, whereas certain regions of Jharkhand and West Bengal demonstrate low trend values (~ -2 W/m^2 per season/year). The SHF trend values at 2100 UTC varies between -0.2–0.2 W/m^2 per season/year. For LHF trend values, at 0900 UTC, which are quite opposite to SHF pattern, higher trend values exist over parts of Jharkhand and West Bengal (~ 4 W/m^2 per season/year), but negative trend values are shown in other regions (~ -4 W/m^2 per season/year). There is no significant trend in LHF variability for 2100 UTC with values varying between -0.2 to 0.2 W/m^2 per season/year.

(*iii*) CAPE analysis conducted at 0900 and 2100 UTC shows that mean values decrease as one move from the coastal to inland regions. Inland regions exhibit trend values that are nearly zero. However, at 0900 UTC, coastal areas exhibit predominantly high positive trends, but at 2100 UTC, a notable high negative trend is observed. For CIN, the values are higher for the coastal regions at 0900 UTC but substantially decrease as one move inland. However, 2100 UTC CIN values are higher than previously reported threshold values of 150 J/kg (Tyagi *et al.*, 2011) over the whole region, and do not support thunderstorm activities in general. The CIN data indicates a mixed trend pattern at 0900 UTC, however, by 2100 UTC, the coastal regions exhibit a positive trend, while most places display a low or less significant trend.

(*iv*) A strong positive connection is observed at 0900 UTC between SHF–CAPE and most regions, especially in inland regions. However, around 2100 UTC, the results demonstrate a negative association. For both 0900 and 2100 UTC, the LHF–CAPE correlations are positive and low for coastal regions. But when it comes to inland regions 0900 UTC shows negative correlations, but 2100 UTC is showing positive correlations. It is observed that inland areas, especially Odisha, have a noteworthy positive correlation between surface SHF and CIN around 0900 UTC. Coastal regions and parts of West Bengal with a few regions in Jharkhand exhibit a negative correlation in this regard. At 2100 UTC, most regions exhibit a positive correlation between SHF and CIN. When comparing the correlation values of LHF–CIN at

0900 UTC, it is observed that they exhibit opposite correlation values to that of SHF–CIN mostly, at 2100 UTC, the LHF–CIN correlation values are good positive for almost all regions.

(*v*) In this study, the analysis is constrained to two specific UTC hours (0900 and 2100 UTC), selected based on the typical diurnal variation in convective activity, with a focus on time periods corresponding to relatively stronger and weaker convection. Additionally, the spatial domain is limited to regions more susceptible to thunderstorm occurrences during the pre-monsoon season. Furthermore, vertical atmospheric profiles have not been considered in the present analysis.

(*vi*) Another limitation of this study is the exclusion of a detailed investigation into the influence of other potentially relevant atmospheric variables.

(*vii*) Further analysis, including a broader set of thermodynamic and dynamic parameters may provide deeper insights into the mechanisms governing convective variability.

(viii) The scope of the present study can be expanded in future work to encompass additional seasons (*e.g.*, monsoon and post-monsoon) and extended temporal and spatial coverage across multiple years. Also incorporating vertical structure information to enable a more comprehensive understanding of convective processes. Furthermore, the application of numerical weather prediction models to simulate surface sensible and latent heat fluxes, and thermodynamic variables-along with a comparison against observational datasets-remains an important avenue for future research.

Data availability

The ERA5 data used in the present study are obtained from the website (https://cds.climate.copernicus.eu/datasets/reanalysis-era5-single-levels?tab=download)

Funding Statement

This research received no specific grant from any funding agency.

Code availability

Code will be made available as per requirements.

Acknowledgements

The author want to acknowledge the National Institute of Technology Rourkela for providing research facilities to conduct this research.

Authors' Contributions

Abheendra Bandary: Performed the data analysis, initial draft. (*email - abheendra1998@gmail.com*).
Rajesh Kumar Sahu: Performed data analysis (*email - rsahu657@gmail.com*).
Bhishma Tyagi: Conceptual design, supervision, manuscript iteration.
All the authors have read and approved the final manuscript.

Disclaimer: The contents and views expressed in this study are the views of the authors and do not necessarily reflect the views of the organizations they belong to.

References

Arora, K., Ray, K., Ram, S., and Mehajan, R., 2023, "The Role of Instability Indices in Forecasting Thunderstorm and Non-Thunderstorm Days across Six Cities in India", *Climate*, **11**, 1, 14.

Benítez-Valenzuela, L. I. and Sanchez-Mejia, Z. M., 2020, "Observations of turbulent heat fluxes variability in a semiarid coastal lagoon (Gulf of California)", *Atmosphere*, **11**, 6, 626.

Bhat, G. S., 2001, "Near surface atmospheric characteristics over the North Bay of Bengal during the Indian summer monsoon", *Geophysical Research Letters*, **28**, 6, 987-990.

Braham, R.R., 1952, "The water and energy budgets of the thunderstorm and their relation to thunderstorm development", *Journal of Atmospheric Sciences*, **9,** 4, 227-242.

Chakraborty, T., Pattnaik, S., Vishwakarma, V. and Baisya, H., 2021, "Spatio-temporal variability of pre-monsoon convective events and associated rainfall over the State of Odisha (India) in the recent decade", *Pure and Applied Geophysics*, **178**, 11, 4633-4649.

Chen, X., Su, Z., Ma, Y., Liu, S., Yu, Q. and Xu, Z., 2014, "Development of a 10-year (2001–2010) 0.1 data set of land-surface energy balance for mainland China", *Atmospheric Chemistry and Physics*, **14**, 23, 13097-13117.

Danodia, A., Sehgal, V. K., Mukherjee, J., Das, D. K. and Patel, N., 2018, "Diurnal and seasonal patterns of sensible and latent heat fluxes from irrigated agroecosystem by large aperture scintillometry", *Journal of Agrometeorology*, **20**, 03, 102–6.

DeMott, C. A. and Randall, D. A., 2004, "Observed variations of tropical convective available potential energy", *Journal of Geophysical Research: Atmospheres*, **109**, (D2).

Duan, A., and Wu, G., 2009, "Weakening trend in the atmospheric heat source over the Tibetan Plateau during recent decades. Part II: Connection with climate warming", *Journal of Climate*, **22**, 15, 4197-4212.

Danodia, A., Sehgal, V. K., Mukherjee, J., Das, D. K. and Patel, N., 2018, "Diurnal and seasonal patterns of sensible and latent heat fluxes from irrigated agroecosystem by large aperture scintillometry", *Journal of Agrometeorology*, **20**, 03, 102–6.

Fisher, R. A., 1934, "Statistical methods for research workers".

Garstang, M., 1967, "Sensible and latent heat exchange in low latitude synoptic scale systems", *Tellus*, **19**, 3, 492-508.

Gensini, V. A., Converse, C., Ashley, W. S. and Taszarek, M., 2021, "Machine learning classification of significant tornadoes and hail in the United States using ERA5 proximity soundings", *Weather and Forecasting*, **36,** 6, 2143-2160.

Ghosh, S., Sen, P. K. and De, U. K., 2004, "Classification of thunderstorm and non-thunderstorm days in Calcutta (India) on the basis of linear discriminant analysis", *Atmósfera*, **17**, 1, 1-12.

Gogoi, P. P., Vinoj, V., Swain, D., Roberts, G., Dash, J. and Tripathy, S., 2019, "Land use and land cover change effect on surface temperature over Eastern India", *Scientific Reports*, **9**, 1, 8859.

Gutzler, D. S., 1992, "Climatic variability of temperature and humidity over the tropical western Pacific", *Geophysical Research Letters*, **19**, 15, 1595-1598.

Hamed, K. H. and Rao, A. R., 1998, "A modified Mann-Kendall trend test for autocorrelated data. *Journal of hydrology"*, **204**, 1-4, 182-196.

Hamed, K. H., 2009, "Exact distribution of the Mann–Kendall trend test statistic for persistent data", Journal *of Hydrology*, **365**, 1-2, 86-94.

Hersbach, H., Bell, B., Berrisford, P., Hirahara, S., Horányi, A., Muñoz-Sabater, and Thépaut, J. N., 2020, "The ERA5 global reanalysis," *Quarterly Journal of the Royal Meteorological Society*, **146**, 730, 1999-2049.

Hirsch, R. M., Alexander, R. B. and Smith, R. A., 1991, "Selection of methods for the detection and estimation of trends in water quality," *Water Resources Research*, **27**, 5, 803-813.

Hughes, C. P. and Veron, D. E, 2018, "A characterization of the Delaware sea breeze using observations and modeling". *Journal of Applied Meteorology and Climatology*, **57**, 7, 1405-1421.

Keenan, T. D., Ferrier, B. and Simpson, J., 1994, "Development and structure of a maritime continent thunderstorm", *Meteorology and Atmospheric Physics*, **53**, 3-4, 185-222.

Laird, N. F., and Kristovich, D. A., 2002, "Variations of sensible and latent heat fluxes from a Great Lakes buoy and associated synoptic weather patterns", *Journal of Hydrometeorology*, **3,** 1, 3-12.

Mahto, S. S. and Mishra, V., 2019, "Does ERA-5 outperform other reanalysis products for hydrologic applications in India?" *Journal of Geophysical Research: Atmospheres*, **124**, 16, 9423-9441.

Mann, H. B., 1945, "Mann Nonparametric test against trend", *Econometrica.*

Martens, B., Schumacher, D. L., Wouters, H., Muñoz-Sabater, J., Verhoest, N. E. and Miralles, D.G., 2020, "Evaluating the land-surface energy partitioning in ERA5", *Geoscientific Model Development*, **13,** 9, 4159-4181.

Martínez-Alvarez, V., Gallego-Elvira, B., Maestre-Valero, J. F., and Tanguy, M., 2011, "Simultaneous solution for water, heat and salt balances in a Mediterranean coastal lagoon (Mar Menor, Spain)", *Estuarine, Coastal and Shelf Science*, **91**, 2, 250-261.

Matalas, N. C. and Sankarasubramanian, A., 2003, "Effect of persistence on trend detection via regression", *Water Resources Research*, **39**, 12.

Murthy, B. S. and Sivaramakrishnan, S., 2006, "Moist convective instability over the Arabian Sea during the Asian summer monsoon", *Meteorological Applications*, **13**, 1, 63-72.

Murugavel, P., Pawar, S. D. and Gopalakrishan, V., 2014, "Climatology of lightning over Indian region and its relationship with convective available potential energy", *International Journal of Climatology*, **34**, 11, 3179-3187.

Murugavel, P., Pawar, S. D. and Gopalakrishnan, V., 2012, "Trends of Convective Available Potential Energy over the Indian region and its effect on rainfall", *International Journal of Climatology*, **32**, 9**.**

Nordbo, A., Launiainen, S., Mammarella, I., Leppäranta, M., Huotari, J., Ojala, A. and Vesala, T., 2011, "Long-term energy flux measurements and energy balance over a small boreal lake using eddy covariance technique", *Journal of Geophysical Research: Atmospheres*, **116,** D2.

Patnaik, U., Das, P. K. and Bahinipati, C. S., 2013, "Analyzing vulnerability to climatic variability and extremes in the coastal districts of Odisha, India", *Review of Development and Change*, **18**, 2, 173-189.

Peel, M. C., Finlayson, B. L. and McMahon, T. A., 2007, "Updated world map of the Köppen-Geiger climate classification", *Hydrology and Earth System Sciences*, **11,** 5, 1633-1644.

Riemann-Campe, K., Fraedrich, K. and Lunkeit, F., 2009, "Global climatology of convective available potential energy (CAPE) and convective inhibition (CIN) in ERA-40 reanalysis", *Atmospheric Research*, **93**, 1-3, 534-545.

Roy Bhowmik, S. K., Sen Roy, S. and Kundu, P. K., 2008, "Analysis of large-scale conditions associated with convection over the Indian monsoon region", *International Journal of Climatology: A Journal of the Royal Meteorological Society*, **28**, 6, 797-821.

Sahu, R. K., Dadich, J., Tyagi, B., Vissa, N.K. and Singh, J., 2020a. "Evaluating the impact of climate change in threshold values of thermodynamic indices during pre-monsoon thunderstorm season over Eastern India", *Natural Hazards*, **102**, 3, 1541-1569.

Sahu, R.K., Dadich, J., Tyagi, B. and Vissa, N.K., 2020b. "Trends of thermodynamic indices thresholds over two tropical stations of north-east India during pre-monsoon thunderstorms", *Journal of Atmospheric and Solar-Terrestrial Physics*, **211**, 105472.

Sahu, R., Tyagi, B., Vissa, N. and Mohapatra, M., 2022a "Pre-monsoon thunderstorm season climatology of Convective Available Potential Energy (CAPE) and Convective Inhibition (CIN) over Eastern India" *Mausam*, **73**, 3, 565–586.

Sahu, R.K., and Tyagi, B., 2022b, "Spatial variation of thermodynamic indices over north-east India during pre-monsoon thunderstorm season", *Journal of Atmospheric and Solar-Terrestrial Physics*, **232**, 105868.

Samanta, S., Tyagi, B., Vissa, N.K. and Sahu, R.K., 2020, "A new thermodynamic index for thunderstorm detection based on cloud base height and equivalent potential temperature", *Journal of Atmospheric and Solar-Terrestrial Physics*, **207**, 105367.

Satyanarayana, A.N.V., Sultana, S., Rao, T. N. and Kumar, S. S., 2014, "Evaluation of atmospheric turbulence, energy exchanges and structure of convective cores during the occurrence of mesoscale convective systems using MST radar facility at Gadanki", *Atmospheric Research*, **143**, 198-215.

Schober, P., Boer, C., and Schwarte, L. A., 2018, "Correlation coefficients: appropriate use and interpretation," *Anesthesia & Analgesia*, **126,** 5, 1763-1768.

Sen, P. K., 1968, "Robustness of some nonparametric procedures in linear models", *The Annals of Mathematical Statistics*, 1913-1922.

Tirkey, A. S., Ghosh, M., Pandey, A. C. and Shekhar, S., 2018, "Assessment of climate extremes and its longterm spatial variability over the Jharkhand state of India", *The Egyptian Journal of Remote Sensing and Space Science*, **21**, 1, 49-63.

Tyagi, B. and Satyanarayana, A.N.V., 2015, "Delineation of surface energy exchanges variations during thunderstorm and non-thunderstorm days during pre-monsoon season", *Journal of Atmospheric and Solar-Terrestrial Physics*, **122,** 138-144.

Tyagi, B., Satyanarayana, A.N.V., Rajvanshi, R. K. and Mandal, M., 2014, "Surface energy exchanges during pre-monsoon thunderstorm activity over a tropical station Kharagpur", *Pure and applied Geophysics*, **171**, 7, 1445-1459.

Tyagi, B., Naresh Krishna, V. and Satyanarayana, A.N.V., 2011, "Study of thermodynamic indices in forecasting pre-monsoon thunderstorms over Kolkata during STORM pilot phase 2006–2008", *Natural hazards*, **56**, 681-698.

Tyagi, B., Sahu, R. K., Hari, M. and Vissa, N. K., 2022, "Thermodynamic changes in the atmosphere associated with pre-monsoon thunderstorms over eastern and north-eastern India", *Extreme Natural Events: Sustainable Solutions for Developing Countries*, 165-197.

Tyagi, B., Satyanarayana, A. N. V., Kumar, M., and Mahanti, N. C., 2012, "Surface energy and radiation budget over a tropical station: an observational study", *Asia-Pacific Journal of Atmospheric Sciences*, **48**, 411-421.

Vissa, N.K. and Tyagi, B., 2021, "Aerosol dipole pattern over India: consequences on rainfall and relation with wind circulations", *Acta Geophysica*, **69**, 2475-2482.

Westermayer, A. T., Groenemeijer, P., Pistotnik, G., Sausen, R. and Faust, E., 2017, "Identification of favorable environments for thunderstorms in reanalysis data", *Meteorologische Zeitschrift*, **26**, 59–70.

Yang, K., Guo, X. and Wu, B., 2011, "Recent trends in surface sensible heat flux on the Tibetan Plateau", *Science China Earth Sciences*, **54**, 1, 19-28.

Zhang, G. J., 2002, "Convective quasi-equilibrium in midlatitude continental environment and its effect on convective parameterization", *Journal of Geophysical Research: Atmospheres*, **107,** D14, ACL-12.